Intraslab Seismicity and Seismic Structure of the Northern Cascadia Subduction Zone

Annual Summary: USGS NEHRP External Grant 02-HQ-GR-0045 November 2003

Michael G. Bostock & Todd A. Nicholson

Department of Earth and Ocean Sciences, The University of British Columbia
147-2219 Main Mall, Vancouver, B.C., Canada, V6T 1Z4
Tel: 604-822-2449; Fax 604-822-6088; email: bostock@eos.ubc.ca

NEHRP Element III (PN)

Key Words: Seismology, Wave propagation, Seismotectonics, Reflection seismology

Investigations Undertaken

This grant is to support work on the structure of the Cascadia subduction zone and its controls on earthquake hazard in the Pacific Northwest. It provides partial funding for a post-doctoral fellow, research technician, and logistical costs of field operations in support of the acquisition, processing and interpretation of data from a portable array of three-component broadband seismometers located in southwestern British Columbia and northwestern Washington. Here we present results from the processing of scattered waves in the teleseismic *P*-coda from some 40 distant earthquakes recorded at both portable and permanent 3-component broadband stations over the region. We then proceed to examine the implications of these results for our understanding of the structure and geometry of the subducting Juan de Fuca plate.

Results

Deployment of 26 temporary broadband stations on a quasi-linear profile that traverses southern Vancouver Island, northwest Washington state and the upper Fraser Valley began in April 2002 and was completed by early 2003. These stations are complemented by another 5 stations along the same profile that are operated by the Geological Survey of Canada and approximately 10 more in the general region operated by the Geological Survey of Canada and the University of Washington. The locations and names of stations employed in this work are shown in figure 1. From these stations we have assembled a data set of teleseismic *P*-waveforms from some 40 distant earthquakes that have occurred over the period June 2002 through November 2003 to investigate the structure of the subducting plate. Examples of seismograms from a single event (see figure 2) show clear signatures from the subducting plate including both forward and back scattered wave energy. Our primary motivation in this work is to use the scattered signals to 1) better constrain the location of the plate interface (top of subducting oceanic plate) for studies of seismic hazard from great thrust earthquakes; and 2) to investigate the signature of slab dehydration that is likely responsible for Wadati Benioff (deep) events and may provide controls on the down-dip rupture limit of thrust earthquakes. To this point we have used two complementary approaches to model plate structure, namely a) a non-linear, directed search algorithm to accurately determine the orientation of the shallow

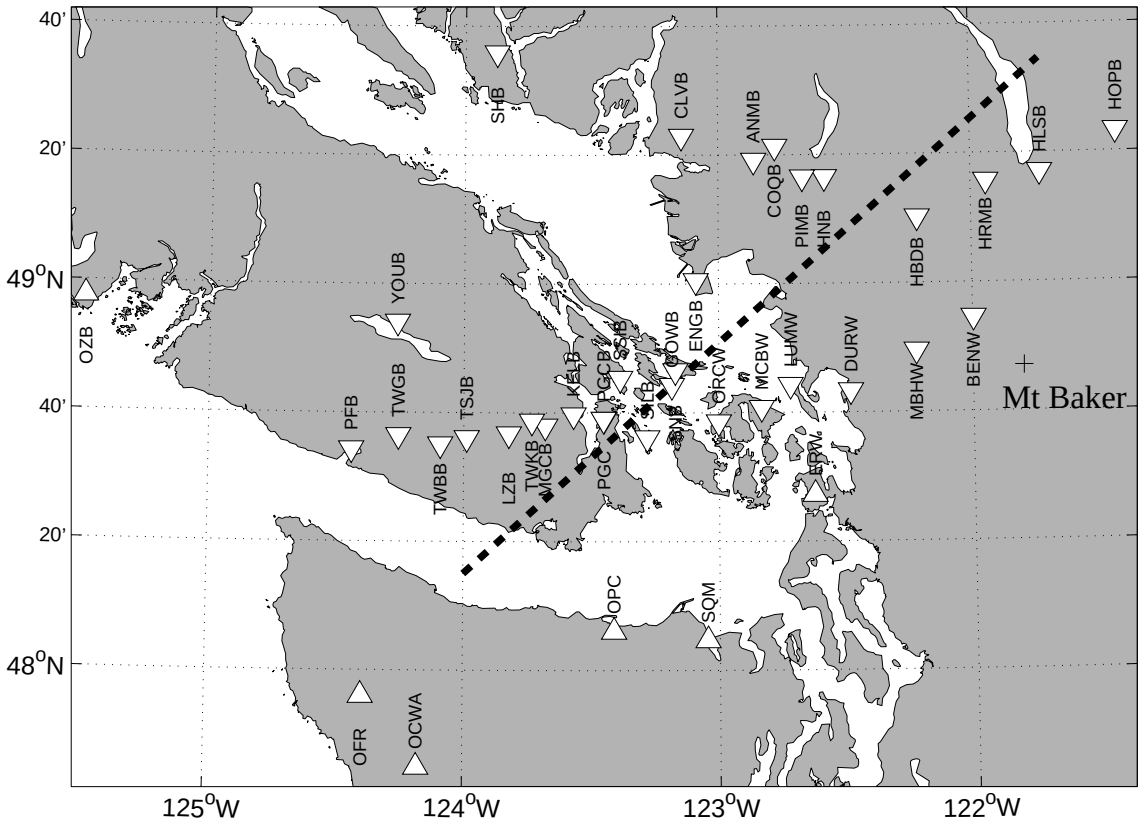

Figure 1: Distribution of broadband, three-component stations over northern Cascadia. Stations used in a linearized inversion representing structure along the 2-D dip-profile (dashed line) are shown as inverted trianges; other stations are shown as upright triangles.

plate; and b) a linearized, 2-D waveform inversion for detailed structure across a 2-D profile shown in figure 1 (dashed line). The results from these efforts are elaborated upon below.

1. Neighbourhood inversion for shallow plate geometry

The first approach we take to modelling data such as those shown in figure 2 involves a non-linear inversion for the geometric properties of the shallow slab. We use the forward-modelling algorithm of Frederiksen and Bostock (2000) wherein synthetic seismograms are generated for Earth models comprising stacks of planar, dipping layers. This forward modelling engine is employed within the neighbourhood inversion algorithm of Sambridge (1999) to efficiently search through a large ensemble of models and extract those that provide the closest matches to the data. The approach is applied in two ways.

First, we consider only those stations from southern Vancouver Island that lie in close proximity to the 2-D profile shown in figure 1. The plate signature in this region is well defined (see figure 2) and, at low frequencies, accurately modelled in terms of planar, dipping layers. In particular we note that the scattered signals in figure 2 appear to originate from a low-velocity layer that parallels the expected dip of subducting plate and which we take for the present to be the oceanic crust. We constrain the shallow layers above the slab to conform to the velocity model used by the Geological Survey of Canada (John Cassidy, pers.

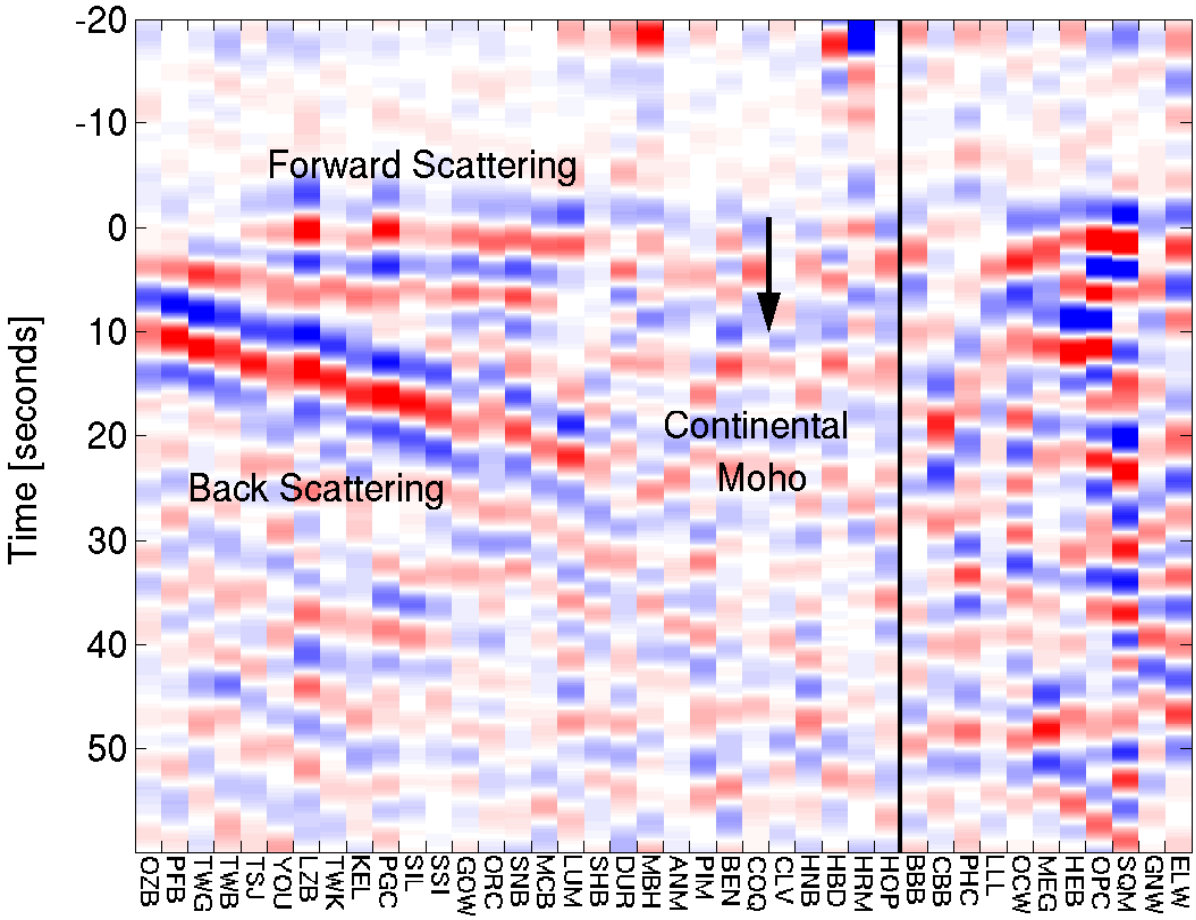

Figure 2: Source-normalized scattered S-waves (or "receiver-functions") for the June 16, 2003 Mw 6.3 event in Kamchatka recorded on the stations in figure 1. Stations OZB to HOPB are plotted in approximately down-dip order; stations BBB to ELW are stations off the main profile (dashed line in figure 1) and arranged in no particular order. Clear forward- and back-scattered signals from a low-velocity layer within the subducting oceanic plate are apparent with a weak continental Moho expressed at the eastern end of the profile.

comm.) to locate earthquakes in the vicinity of Vancouver Island and allow the properties (dip, depth, strike) of the oceanic crust (layer 5 in Table 1) to vary. The parameters for the best fit model incorporating those Vancouver Island stations that fall along the profile are given in Table 1. The synthetic seismograms corresponding to this model are shown in figure 3 and demonstrate that the dominant scattered signal is generated by a ∼8 km thick, low-velocity layer, approximately 20 km deep at the western end of the profile that dips gently at ∼ 17° in a direction N50°E. Both strike and dip correspond closely to slab contour model of Flueck et al. (1997); however, the depths to the inferred top of oceanic crust are, as we discuss below, considerably shallower than those previously published. Synthetic seismograms for this model are plotted in figure 3 and capture the essential characteristics of the data.

In the second application we model data from stations with strong slab signatures individually to recover a local estimate of the depth to the top of layer 5, inferred to be the top of the oceanic crust. These values are plotted in figure 4. together with the depth to top of slab

Table 1: Model parameters for best fit plate model across Vancouver Island. Those values shown with an asterisk are permitted to vary in the inversion; all other parameters are held fixed.

Layer	Thickness (km)	V_P (m/s)	V_S (m/s)	ρ (kg m^{-3}	Strike	Dip
1	1.0	5000	2890	2800	0	0
2	5.0	6000	3460	2800	0	0
3	4.0	6700	3870	3200	0	0
4	9.3	6700	3870	3200	0	0
5	10.0	6500	3500	3000	-42	17.8
6	90.0	7500	4300	3200	0	0

contours of Flueck et al., 1997 (modified slightly by Wang, 2003, pers. comm.), and once more it is evident that the estimated depth to top of crust from the teleseismic data is inconsistent with the published estimates by approximately 10 km at the western end of the profile.

2. 2-D Migration Inversion of structure along the *POLARIS* profile

We now proceed to use the results from the previous section, namely the strike direction of the dipping plate, to map the stations onto an optimal linear profile as required for application of a simultaneous 2-D linearized inversion/migration of the entire teleseismic data set. We use the inversion algorithm of Bostock et al. (2001) that allows events from arbitrary back-azimuths to be inverted under the assumption that the underlying structure perpendicular to the profile is 2-dimensional. This approach has two advantages over the non-linear inversion employed in the previous section: i) the full suite of teleseismic data set can be employed in the inversion (versus a select few events); ii) imaged structures are not constrained to be planar but can assume arbitary geometry (apart from the restriction of 2-dimensionality). Linearized inversion requires the specification of a reference (background) model that accurately accounts for the propagation characteristics of the incident and scattered wavefields. Consequently, we have once more adopted the 1-D model used by the Geological Survey of Canada in their earthquake relocations as represented by the layers 1-3,6 in Table 1. Because converted (*P*-to-*S*) scattered waves are most sensitive to variations in shear moduli, we have cast our inversion in terms of the recovery of *S*-velocity perturbations. In this context a normal discontinuity, such as the continental Moho, will appear as a rapid transition between low velocity (red) to high velocity (blue).

The model shown in the top of figure 5 represents the inversion of *Pps* waveforms from 41 high-quality events. On the western end of the profile (which coincides with station PFB on the west coast of Vancouver Island), we see the signature of the inferred oceanic crust as a low-velocity (red) layer of thickness $\sim$ 10 km dipping at 17 degrees to the northeast. The dip and depth of the crust as determined from the non-linear inversion of the previous section are in good agreement with the model in this figure. The thickness of the crustal layer in the linearized inversion is, however, somewhat overestimated as a result of the interference of two back scattered phases that arrive in close succession (namely, the *Pps* phase from the oceanic Moho and the *Pss* phase from the top of the oceanic crust). This artifact is a consequence of the linearized inversion and is not a factor in the analysis of the previous section. The nature of the interference is such that we would expect the top of the crust to be better resolved in depth

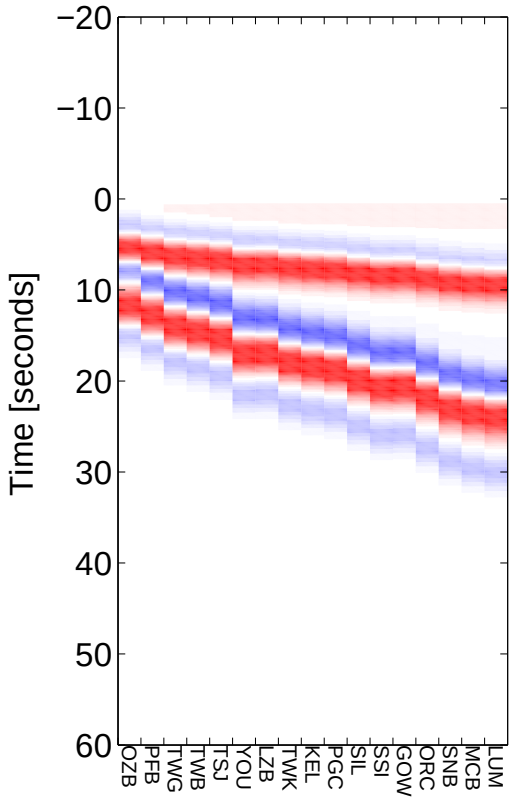

Figure 3: Synthetic seismograms corresponding to the data in figure 2 for a model that fits data from Vancouver Island stations. The earlier arrival (blue-red) arrival represents forward scattered waves from a low-velocity layer; the later arrival (blue-red-blue) is actually the superposition of two free-surface, reflected back-scattered arrivals from the same layer.

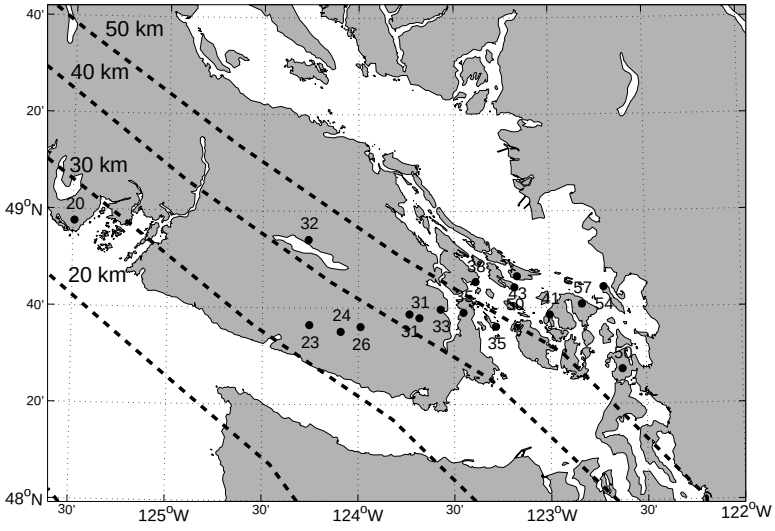

Figure 4: Depths to top of low-velocity layer (interpreted to be oceanic crust) relative to depth contours from Flueck et al. (1997). Note the discrepancy of $\sim$ 10 km for most stations on Vancouver Island.

than its base. There is the suggestion of a "bump" at the top of the oceanic crust near 30 km distance along the profile that does not exhibit an obvious counterpart in Moho topography. At ∼80 km along the profile coinciding approximately with the east coast of Vancouver Island, the top of the crust appears to flatten out and its associated velocity contrast undergoes a dramatic reduction. The oceanic Moho can, however, be traced to a depth of 60 km to a point ∼140 km northeast along the profile. The last station on the profile is HOPB at the mouth of the Fraser Valley and approximately 180 km along the profile. The "smiles" in the image generated at that point and farther to the northeast result from a lack of station coverage in that direction causing a smearing of energy along pseudo-elliptical curves in space.

The signature observed along this profile is similar to that observed further south along a comparable profile in central Oregon. The *Pps* image for that profile is shown to the same scale in the lower part of figure 5. The basic elements of both images are similar and can be interpreted in the following way, as suggested by Bostock et al. (2001). The abrupt reduction in *S*-velocity contrast in the oceanic crust at depths near 40 km is due to transformation of basaltic minerals within the subducting oceanic crust to eclogite. This process is expected to release significant quantities of water into the cool, overlying mantle wedge producing lower seismic velocities through serpentinization (Bostock et al., 2001; Brocher et al., 2003). In Oregon, this process is so effective that it has apparently reduced velocities near the wedge corner to the extent that they are lower than those in the overlying crust, producing an inverted continental Moho. Regular polarity continental Moho (*i.e.* low-velocity above/high velocity below) is apparent only on the eastern edge of the profile between 150-250 km. In northern Cascadia (top panel in figure 5) the velocity reduction is not quite as extreme but, as there is no clear expression of the continental Moho, any associated *S*-velocity contrast must be small. The shorter length of the northern Cascadia profile causes the reappearance of the Moho to be obscured by the "smiles" artifacts mentioned above, but a Moho signature is becoming evident by, again, 150 km along the profile at a depth of 34 km. Finally we note that the geometry of the plate across Oregon differs from that below Vancouver Island. Specifically, the dip of the southern plate appears to increase with depth, whereas that for the northern plate is more constant, in contrast once more to the depth contours in figure 4.

Future Work

The results presented above are preliminary and raise an important issue that must be addressed and resolved before detailed analysis of plate structure and Wadati-Benioff seismicity is undertaken. The principal dilemna concerns the depth contours to the low velocity layer that we have interpreted to be oceanic crust. Both the non-linear and linear inversions suggest that the top of crust is ∼10 km shallower below western Vancouver Island than generally assumed and more closely coincident with the so-called "E" layer identified in Lithoprobe reflection studies (*e.g.* Hyndman et al., 1990). An accurate knowledge of the location/geometry of the subducting plate is clearly important for earthquake hazard assessment. Over the next few months, we shall devote our efforts to resolving this contradiction and investigating the relation between slab structure and intraplate seismicity. Several factors will be considered in our analysis:

1) The teleseismic data indisputably image a dipping low-velocity layer beneath southern Vancouver Island as evidenced by distinct and characteristic forward and back scattering signatures. These signatures are most coherent at the lower frequencies (< 0.4 Hz) that have been employed in this report. We will examine the characteristics of scattered arrivals at (better re-

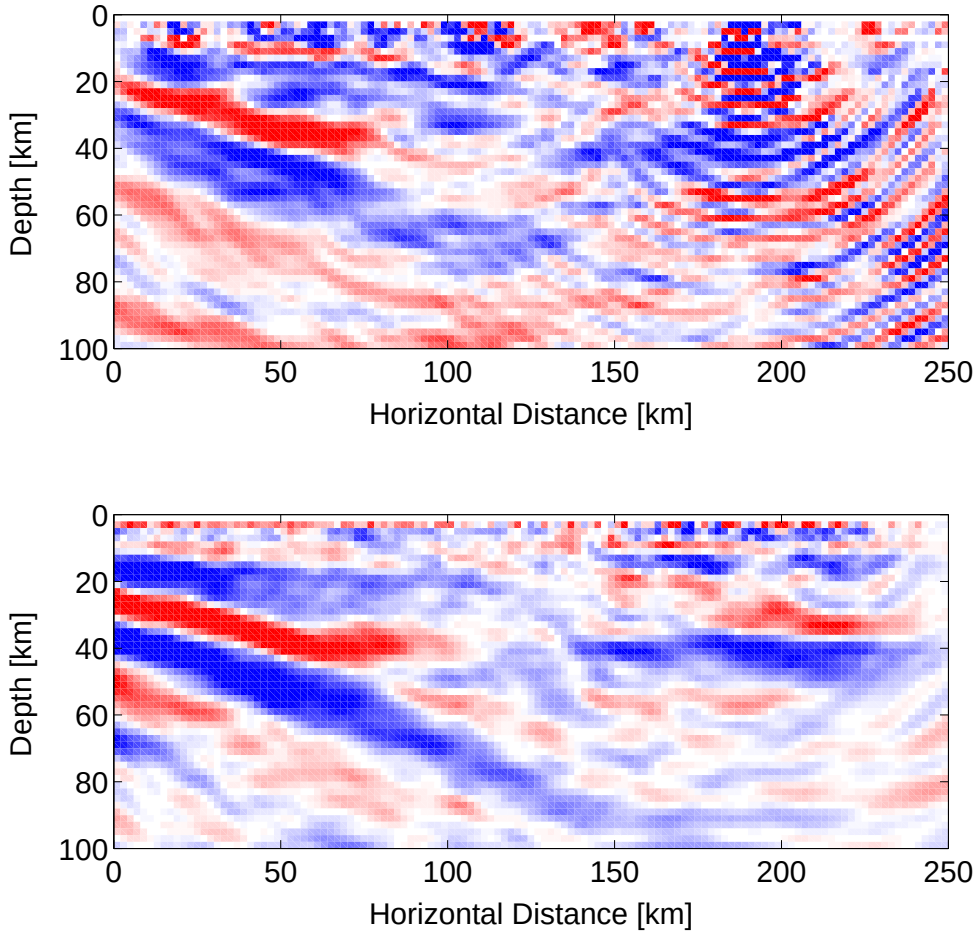

Figure 5: Teleseismic migration images using the scattered *Pps* phase across Cascadia. Top figure shows result from current study across southern Vancouver Island, northwestern Washington and the B.C. lower mainland; whereas lower figure is result across central Oregon from Rondenay et al., 2001. See text for details.

solving) higher frequencies to ascertain whether any structure is evident within the low-velocity layer.

2) The depth-postitioning of the low-velocity layer is dependent upon the velocity model used to map traveltimes to depth. To this point we have used the Geological Survey of Canada earthquake relocation model. In future work we shall examine the increase in velocity required to map the low-velocity to greater depths. Nonetheless, we note that the Geological Survey 1-D model is broadly consistent with recent *P*-wave tomography from SHIPS data (*e.g.* Nedimovic et al., 2003); Preston et al., 2003);

3) Trade-offs exist between the thickness of the low-velocity layer and its constitutent velocities and the latter also play a role in determining the amplitude of the scattering (through transmission and reflection coefficients). We have yet to tightly constrain the thickness of the low-velocity layer and so, in principle, it is conceivable that the low-velocity layer layering might include both the "E"-layer and oceanic crust. We will examine this possibility through more detailed forward and inverse modelling.

4) It is clear from figure 5 that the essential, large-scale structural elements of the subduction zone below Oregon and northern Cascadia, as imaged by scattered teleseismic waves are, fundamentally similar. Thus any valid interpretation of the structures observed in the north must apply equally to central Oregon.

Non-technical Summary

In this report, we have presented preliminary results from studies of subduction zone structure in the Pacific Northwest beneath northwestern Washington and southwestern British Columbia. We clearly image a low-velocity zone (apparently the oceanic crust) within the subducting plate system with an expression similar to that of our earlier work across central Oregon. Our estimates of the depth to the top of the plate disagree with previous studies, however, placing it almost 10 km closer to the surface. The potential consequeces of this discrepancy harbour important implications for earthquake hazard and we will work to resolve the issue over the next few months.

Data Availability

Data from POLARIS stations in British Columbia are available in SEED format and can be acquired through the AutoDRM of the Canadian National Earthquake Hazards Program (contact Jim Lyons at `lyons@seismo.nrcan.gc.ca` for further information). SEED data from stations in Washington state are available via personal request from the author at `bostock@eos.ubc.ca`.

References

Bostock, M.G., Shragge, J., Rondenay, S. Multi-parameter 2-D inversion of scattered teleseismic body waves I - Theory for oblique incidence, *J. Geophys. Res.*, 107, 30771-30778, (2001).

Bostock, M.G., Hyndman, R.D., Rondenay, S., Peacock S.M. An inverted continental Moho and the serpentinization of the forearc mantle, *Nature*, **417**, 536-538, 2002.

Brocher, T.M., Parsons, T., Trehu, A.M., Crosson, R.S., Snelson, C.M., and Fisher, M.A. Seismic evidence for widespread serpentinized forearc upper mantle along the Cascadia

margin, *Geology*, 31, 267-270, 2003.

Clowes, R.M., Brandon, M.T., Green, A.G., Yorath, C.J., Brown, A.S., Kanasewich, E.R., Spencer, C. LITHOPROBE-southern Vancouver Island: Cenozoic subduction complex imaged by deep seismic reflection, *Can. J. Earth Sci.*, **24**, 31-51, 1987.

Flueck, P., R. Hyndman, and K. Wang 3-D dislocation model for great earthquakes of the Cascadia subduction zone, *J. Geophys. Res.*, **102**, 20539-20550, 1997.

Frederiksen, A.W., Bostock, M.G. Modelling teleseismic waves in dipping anisotropic structures, *Geophys. J. Int.*, 141, 401-412, 2000.

Hyndman, R.D., Yorath, C.J., Clowes, R.M., Davis, E.E. The northern Cascadia subduction zone at Vancouver Island: seismic structure and tectonic history, *Can. J. Earth Sci.*, 27, 313-329, 1990.

Nedimovic, M.R., Hyndman, R.D., Ramachandran, K., Spence, G.D. Reflection signature of seismic and aseismic slip on the northern Cascadia subduction interface, *Nature*, 424, 416-420, 2003.

Preston, L. A., Creager, K.C., Crosson, R.S., Brocher, T.M., Trehu, A.M. Intraslab earthquakes: dehydration of the Cascadia slab, *Science*, 1197-1200, 302, 2003.

Sambridge, M. Geophysical Inversion with a neighbourhood algorithm -I. Searching a parameter space, *Geophys. J. Int.*, 138, 479-494, 1999.

Rondenay, S., Bostock, M.G., Shragge, J. Multiparameter two-dimensional inversion of scattered teleseismic body waves, 3. Application to the Cascadia 1993 data set, *J. Geophys. Res.*, **106**, 30795-30807, 2001.